

# 1550 nm external cavity diode laser with enhanced SMSR based on polarization mismatch by grating rotation

YAN WANG,<sup>1,2</sup> HAO WU,<sup>2,\*</sup> XING ZHANG,<sup>1</sup> JIANGUO LIU,<sup>3</sup> CHAO CHEN,<sup>1</sup> YUBING WANG,<sup>1</sup> YINLI ZHOU,<sup>1</sup> LEI LIANG,<sup>1</sup> JUN ZHANG,<sup>1</sup> LI QIN,<sup>1</sup> AND LIJUN WANG<sup>1</sup>

<sup>1</sup>State Key Laboratory of Luminescence and Applications, Changchun Institute of Optics, Fine Mechanics and Physics, Chinese Academy of Sciences, Changchun 130033, China

<sup>2</sup>Daheng College, University of Chinese Academy of Sciences, Beijing 100049, China

<sup>3</sup>Institute of Semiconductors, Chinese Academy of Sciences, Beijing 100083, China

\*Corresponding author: hwu@ciomp.ac.cn

Received 26 April 2019; revised 7 June 2019; accepted 7 June 2019; posted 7 June 2019 (Doc. ID 366164); published 27 June 2019

**A tunable external cavity diode laser (ECDL) with high side-mode suppression ratio (SMSR) is demonstrated. The ECDL is operated at both strong and weak feedback steady states with single longitudinal mode. Compared with the strong feedback mode, the SMSR of the weak feedback mode is significantly enhanced by rotating the grating along the axis of the incident beam, which changes the polarization orientation versus the grating grooves. The highest SMSR of the weak feedback mode is 54 dB at the injection current of 300 mA. The tunable range of the ECDL with weak feedback mode reaches 130.9 nm. © 2019 Optical Society of America**

<https://doi.org/10.1364/AO.58.005213>

## 1. INTRODUCTION

Optical feedback from an external cavity has significant influence on the characteristics of laser diodes in terms of stability, relative intensity noise, linewidth, tunability, and so on [1–3]. According to the experiments and calculations, there are five feedback regimes depending on the optical feedback intensity [4–6]. At the low feedback level of optical power without anti-reflection (AR) coating, the linewidth is dependent on the phase of the feedback and the cavity length. Laser diodes with AR coating achieve a high feedback level, and the external cavity diode laser (ECDL) can operate on a single longitudinal mode for all phases of the feedback. In general, the optical feedback in the ECDL configuration is used to optimize laser performance measures such as frequency stability, linewidth, and signal-to-noise ratio [7,8]. Optical feedback from a long external cavity formed by a fiber is applied to suppress the high-frequency noise and narrow the Lorentzian linewidth [9]. Modulation bandwidth enhancement of the semiconductor laser is demonstrated by controlling feedback light intensity and phase property [10].

In recent years, many different configurations of ECDL with single output mode have been demonstrated [11–13]. Among the ECDL systems, Littrow configuration is the most common for its characteristics of simplicity, compactness, high efficiency, and broad tunable range [14–18]. For the grating-coupled external cavity system, the polarization mismatch between the grating lines and polarization direction of the

incident beam has a significant influence on the optical feedback. Ding *et al.* compare the performance of Littrow ECDL systems with grating lines perpendicular and parallel to the p–n junction, and the parallel condition shows good performance [19]. Chi *et al.* achieve two output states by using a half-wave plate to switch the polarized direction of the laser beam in the Littrow ECDL configuration, where the output beam with weak feedback mode shows a higher power and the output beam with strong feedback mode shows a wider tuning range [20]. They only take into account conditions in which the grating lines were perpendicular and parallel to the polarization direction of the laser beam, and only a multi-mode optical spectrum is observed in the weak optical feedback mode.

In this paper, a tunable ECDL with high SMSR in the Littrow configuration is demonstrated. The ECDL is operated at both strong and weak feedback steady states with single longitudinal mode. The strong feedback mode is achieved when the polarization direction of the beam is perpendicular to the groove direction of the grating. Compared with the strong feedback mode, the SMSR of the weak feedback mode is significantly enhanced by the mismatch between the polarized direction of the incident beam and the groove direction of the grating. The highest SMSR of the weak feedback mode is 54 dB at an injection current of 300 mA, and the tunable range is 130.9 nm. The highest SMSR of the strong feedback mode is only 47 dB.

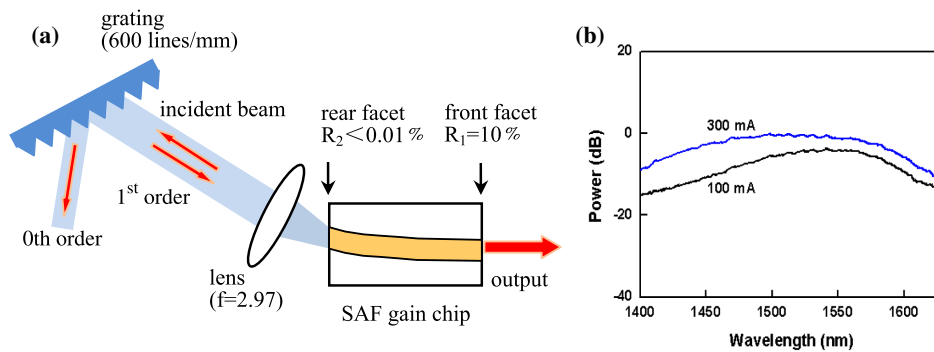


**Fig. 1.** (a) Experimental setup of the Littrow external-cavity diode system. (b) The optical spectra of the SAF gain chip are measured with an injection current of 100 and 300 mA at 20°C.

## 2. EXPERIMENTAL SETUP

Figure 1(a) shows a schematic diagram of the ECDL. The length of the external cavity is about 80 mm. A commercial single angled facet (SAF) gain chip (Thorlabs, SAF1126H heat-sink assembly) sensitive to the transverse electric (TE) mode is used in the Littrow external cavity geometry [21]. The optical spectra of the SAF gain chip are measured with an injection current of 100 and 300 mA at 20°C, as shown in Fig. 1(b). The reflectivity of the angled facet ( $R_2$ ) is less than 0.01%, and the reflectivity of the other facet ( $R_1$ ) is about 10%. The beam from the rear facet is collimated by an aspherical lens of 2.97 mm focal length and a numerical aperture of 0.6 (Thorlabs, 355660-C). The collimated beam is incident on a diffraction grating with a groove density of 600 lines/mm (Thorlabs, GR13-0616) for wavelength selection and optical feedback, and the first-order diffractive beam from the grating is fed back into the gain chip. The output beam is measured from front facet of the gain chip with a constant temperature of 20°C. Two stable external cavity feedback states are realized in the Littrow system, and the switching between the weak and strong feedback is realized by rotating the grating along the axis of the incident beam and first-order diffraction beam of the grating element.

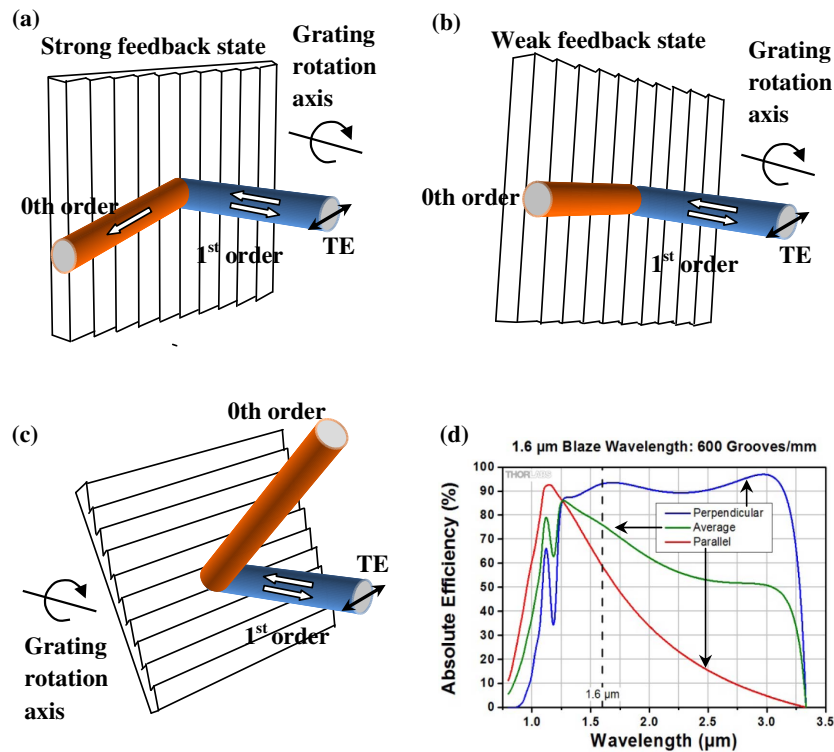
## 3. RESULTS AND DISCUSSION

Figure 2 is the schematic diagram of the grating rotation. Figure 2(a) corresponds to the strong feedback mode with the maximum diffraction efficiency. The polarized direction of the incident beam is perpendicular to the groove direction. When adjusting the grating along the axis of the incident beam, the polarized direction of the incident beam is in an intermediate state between the perpendicular state and parallel state, as shown in Fig. 2(b). Figure 2(b) corresponds to the weak feedback mode. When the polarized direction of the incident beam is parallel to the groove direction, as shown in Fig. 2(c), the diffraction efficiency is the minimum. As shown in Fig. 2(d), the diffraction efficiency varies with different wavelengths with different polarization conditions. The change of the diffraction efficiency results in the change of feedback intensity. Variable feedback steady states can be achieved in the Littrow

configuration by grating rotation along the axis, where grating equation is the essential condition.

The tunability of ECDL systems with weak and strong optical feedback is characterized by measuring the optical spectrum of the output beam at different operating wavelengths. The spectrum was measured by an optical spectrum analyzer (OSA, YOKOGAWA, AQ6370D) with a resolution of 0.02 nm. The measured spectra of the ECDL with weak and strong optical feedback at an injection current of 100 mA are shown in Fig. 3. The tunable ECDL spectra for both states are obtained by adjusting the grating along the groove direction. The tunable spectra of the weak feedback mode, from 1511.9 to 1579.4 nm, are shown in Fig. 3(a). The highest SMSR reaches 48 dB in the central part due to the high active-region gain. Figure 3(b) shows the tunable spectra of the strong feedback mode, from 1500.1 to 1584.1 nm. The highest SMSR is 42 dB. Figures 3(c) and 3(d) are the optical spectra of weak and strong optical feedback, respectively, at the wavelength of 1560 nm. The SMSR of the two feedback modes are 48 and 40 dB, respectively. Figure 4 shows the SMSR of the weak and strong feedback mode with different wavelengths at the current of 100 mA. The ECDL with weak optical feedback can achieve a much higher SMSR. In Fig. 3(d), a gradual mount centered at 1506 nm is observed in the strong feedback mode, which greatly reduces the SMSR. In the weak feedback mode, the gradual mount is thoroughly eliminated. This may be due to the mismatch between the polarized direction of the incident beam and the groove direction of the grating. The observed spectral linewidths of the weak and strong feedback modes are 0.06 and 0.07 nm by the OSA (defined as FWHM), respectively, which is narrower than the free spectral range of the Fabry–Perot (FP) laser cavity (0.3 nm), indicating that the laser system operates in a single longitudinal FP mode. Limited by the OSA, the true linewidth should be much narrower than the observed one.

Figure 5 is the optical spectra of the ECDL system with two optical feedback modes at an injection current of 300 mA. Figure 5(a) shows the spectra of the ECDL from 1455.4 to 1586.3 nm for the weak feedback mode. When the injection current is increased from 100 to 300 mA, the tunable range is increased from 67.5 to 130.9 nm. For the strong feedback mode, the spectra of the ECDL from 1440.6 to 1595.5 nm are shown in Fig. 5(b). The tunable range increases from



**Fig. 2.** Relationship between diffraction efficiency and grating angle. The grating rotation axis is parallel to the incident beam. The relation of the beam polarization axis to the groove direction is (a) perpendicular for the strong feedback mode (polarization match), (b) rotated by  $12^\circ$  (partial mismatched) for the weak feedback mode, and (c) parallel with minimal diffraction efficiency (polarization mismatch). (d) The diffraction efficiency varies with the wavelengths at different polarization conditions in Littrow configuration. Perpendicular: the polarized direction of the incident beam is perpendicular to the groove direction. Parallel: the polarized direction of the incident beam is parallel to the groove direction (Ref. [22]).

84 to 154.9 nm when the current is increased from 100 to 300 mA. According to Fig. 6, the SMSR of the weak feedback mode is much higher. The highest SMSR of the weak and strong feedback modes are 54 and 47 dB, respectively.

Figures 5(c) and 5(d) are the optical spectra of weak and strong optical feedback, respectively, at the wavelength of 1560 nm. The SMSR of the two feedback modes are 52 and 46 dB, respectively.

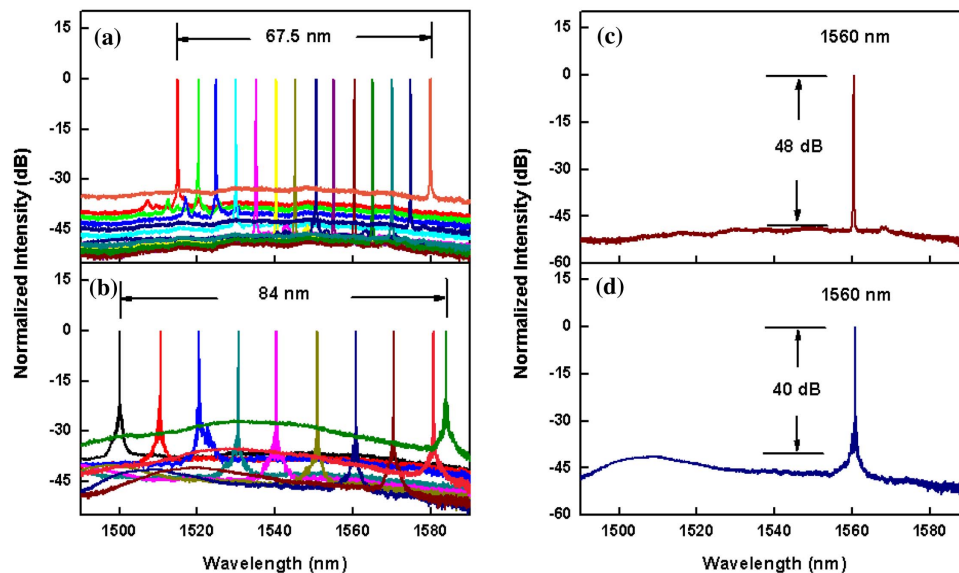


**Fig. 3.** Optical spectra of the output beam from the ECDL system with (a) weak optical feedback and (b) strong optical feedback at  $20^\circ\text{C}$ . (c) and (d) are the optical spectra of the weak and strong optical feedback, respectively, at the wavelength of 1560 nm. The injection current is 100 mA.

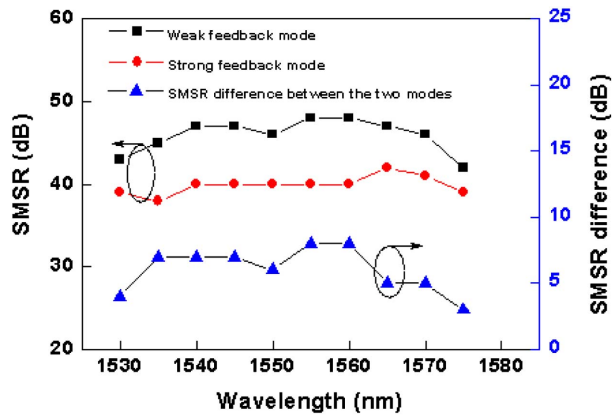


**Fig. 4.** SMSR of the weak and strong feedback mode versus working wavelengths with the current of 100 mA.

Figure 7 is the threshold current of the two feedback modes as a function of the tuning wavelength. The minimum threshold currents of the ECDL system under the strong and weak feedback modes are 50 and 84 mA, respectively. The enhanced optical feedback can effectively decrease the threshold current in the entire tuning range. For the ECDL configuration, the absolute intensity of the optical feedback is difficult to measure. However, it can be estimated from the threshold current ratio of the two feedback modes. We assume a linear relationship between the threshold current and the total optical loss [23]:

$$I_{th} \sim 2\alpha L - \ln R_1 - \ln[R_2 + (1 - R_2)X], \quad (1)$$

where  $L$  is the cavity length of the laser,  $\alpha$  is the effective absorption,  $R_1$  and  $R_2$  are the reflectivity of front and rear facets, and  $X$  is the feedback efficiency. For the ECDL system,

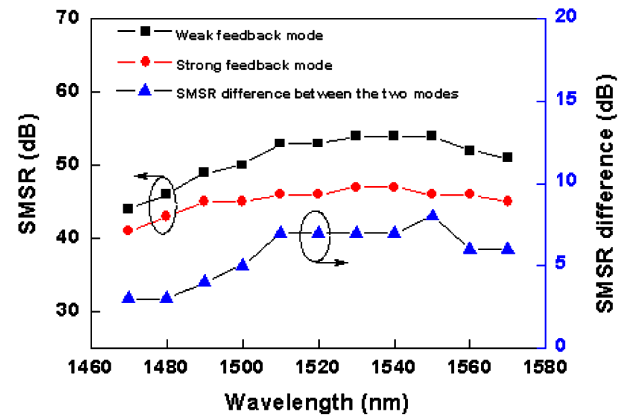


**Fig. 6.** SMSR of the weak and strong feedback mode versus working wavelengths with the current of 300 mA.

$R_2 \ll 1$ . The ratio of thresholds for the two feedback modes is given by

$$\frac{I_{th1}}{I_{th2}} = \frac{2\alpha L - \ln R_1 - \ln X_1}{2\alpha L - \ln R_1 - \ln X_2}, \quad (2)$$

where  $I_{th1}$  and  $I_{th2}$  are the thresholds of the ECDLs with the strong and weak feedback modes. According to the formula, we are able to estimate that the ratio of  $X_1$  and  $X_2$  is about 5.2 at 1560 nm. In this way, we can determine that the feedback efficiency of the weak mode is 19% of the strong mode.

The output power of both feedback modes at different wavelengths is measured by a power meter (Thorlabs, S146C) with an injection current of 300 mA, as shown in Fig. 8. The insets are the output power as a function of the injection current at the wavelength of 1550 nm for both feedback modes. For the weak feedback mode, as shown in Fig. 8(a), the

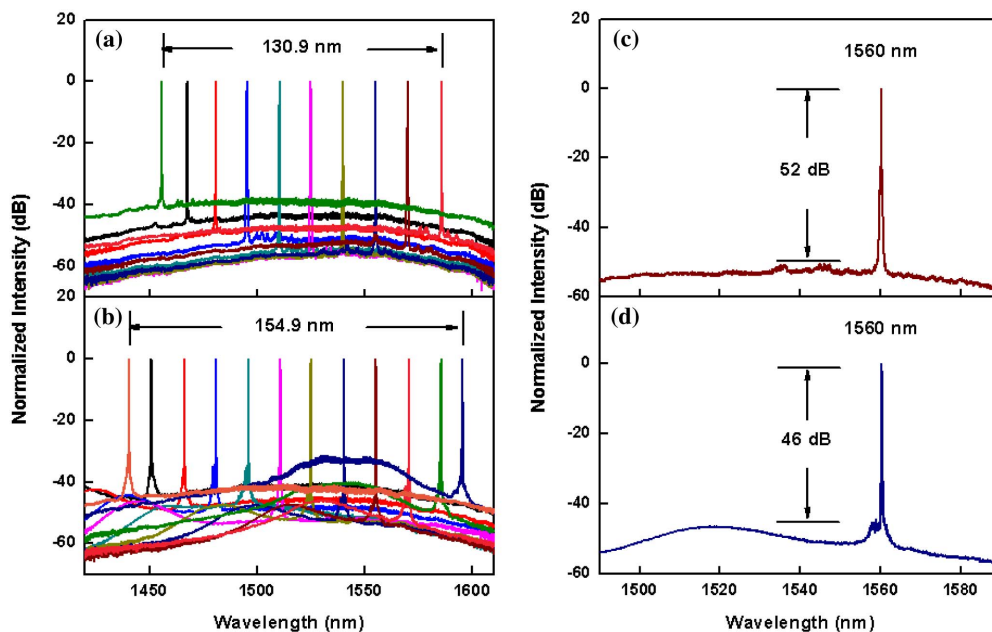


**Fig. 5.** Optical spectra of the output beam from the ECDL system with (a) weak optical feedback and (b) strong optical feedback at 20°C. (c) and (d) are the optical spectra of the weak and strong optical feedback, respectively, at the wavelength of 1560 nm. The injection current is 300 mA.



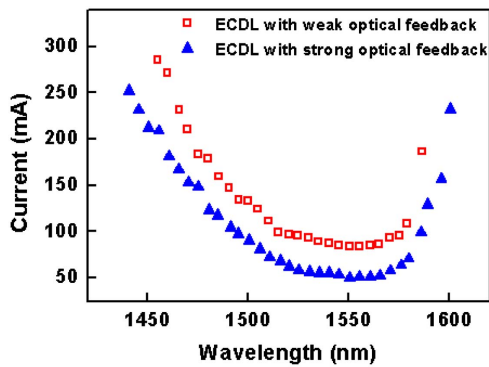


**Fig. 7.** Threshold current is measured as a function of the tuning wavelength for the ECDLs with two feedback modes.

maximum output power is 5.5 mW at 1560 nm. Figure 8(b) shows that the maximum output power of the strong feedback mode is 49.2 mW at 1560 nm. In our experiment, the incident beam can be decomposed into  $x$  components perpendicular to the grating grooves and  $y$  components parallel to the grating grooves, as shown in Fig. 8(c). The gain chip used in the experiment is sensitive to the polarization, which means it can supply optical gain to the TE mode of the feedback beam and almost cannot supply optical gain to the transverse magnetic (TM) mode of the feedback beam. In the weak feedback mode, the polarized direction of the incident beam is non-orthogonal to the groove direction of the grating due to the grating rotation. As shown in Fig. 8(c), the feedback intensity along the  $y$  axis decreases obviously and the feedback intensity along

the  $x$  axis decreases a little, which leads to the drop of optical power of the composed feedback beam. The polarized direction of the feedback beam also rotates, which leads to effective feedback optical power with TE mode matched to the gain chip decreasing further. As a result, the output power of the weak feedback mode decreases significantly.

#### 4. CONCLUSION

In conclusion, based on a Littrow configuration, a tunable ECDL with weak and strong feedback steady states is achieved. The optical spectrum of the weak feedback mode shows enhanced SMSR by rotating the grating along the axis of the incident and first-order diffraction beams of the grating. This may be due to the mismatch between the polarized direction of the incident beam and the groove direction of the grating. When the injection current is 100 and 300 mA, the highest SMSR of the weak feedback mode is 48 and 54 dB, respectively. In contrast, the highest SMSR of the strong feedback mode is only 42 and 47 dB, respectively. This means only the weak feedback mode can achieve SMSR above 50 dB. The tunable range of the ECDL system under the weak feedback mode reaches 130.9 nm. We believe that the weak feedback mode may benefit some specific applications, such as optical sensing, coherent optical communication, and coherent LiDAR, where clean and pure single-frequency optical spectrum with high SMSR is needed. In the future, spectral line-width will be investigated precisely, and a gain chip which is non-sensitive to the polarization will be used in the experiment in order to improve the output power level.

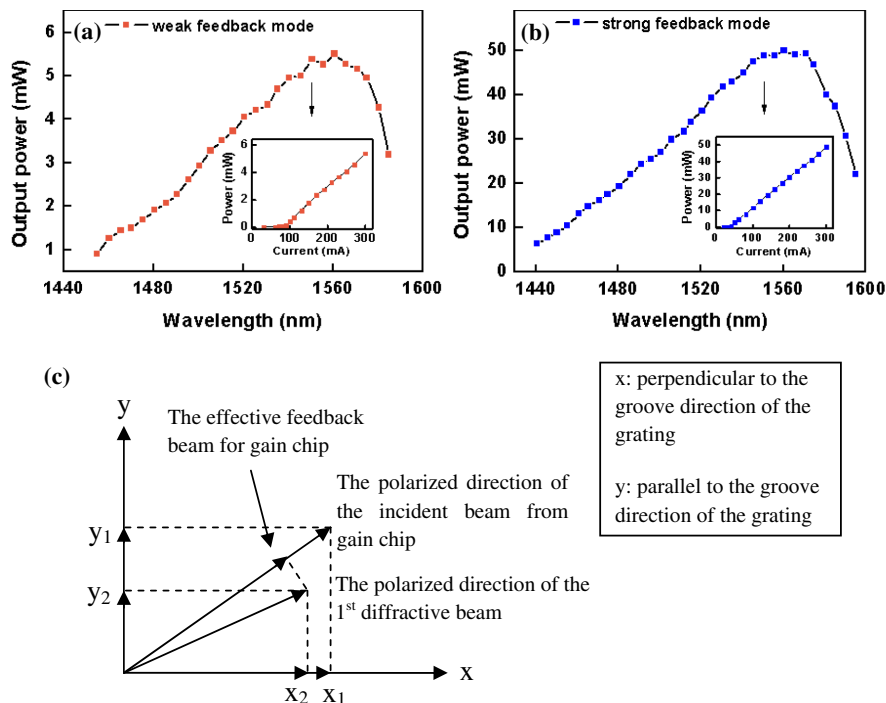


**Fig. 8.** Output power of the ECDL is measured as a function of the wavelength for (a) weak optical feedback and (b) strong optical feedback with an injection current of 300 mA at 20°C. Inset: Output power versus injected current is plotted at a given wavelength of 1550 nm for both modes. (c) Change in the polarized direction of the feedback light for the weak feedback mode.

**Funding.** National Science and Technology Major Project of China (2016YFE0126800); National Natural Science Foundation of China (NSFC) (11774343, 61727822, 61874119); Science and Technology Development Project of Jilin Province (20180201014GX).

## REFERENCES

1. N. Schunk and K. Petermann, "Numerical analysis of the feedback regimes for a single-mode semiconductor laser with external feedback," *IEEE J. Quantum Electron.* **24**, 1242–1247 (1988).
2. J. O. Binder and G. D. Cormack, "Mode selection and stability of a Semiconductor laser with weak optical feedback," *IEEE J. Quantum Electron.* **25**, 2255–2259 (1989).
3. R. Lang and K. Kobayashi, "External optical feedback effects on semiconductor injection laser properties," *IEEE J. Quantum Electron.* **16**, 347–355 (1980).
4. R. Tkach and A. Chraplyvy, "Regimes of feedback effects in 1.5  $\mu\text{m}$  distributed feedback lasers," *J. Lightwave Technol.* **4**, 1655–1661 (1986).
5. K. Kikuchi and T. Okoshi, "Simple formula giving spectrum-narrowing ratio of semiconductor-laser output obtained by optical feedback," *Electron. Lett.* **18**, 10–12 (1982).
6. D. Lenstra, B. Verbeek, and A. J. DenBoef, "Coherence collapse in single mode semiconductor lasers due to optical feedback," *IEEE J. Quantum Electron.* **21**, 674–679 (2003).
7. J. Kitching, R. Boyd, and A. Yariv, "Amplitude noise reduction in semiconductor lasers with weak, dispersive optical feedback," *Opt. Lett.* **19**, 1331–1333 (1994).
8. M. Horstjann, V. Nenakhov, and J. P. Burrows, "Frequency stabilization of blue extended cavity diode lasers by external cavity optical feedback," *Appl. Phys. B* **106**, 261–266 (2012).
9. P. Samutpraphoot, S. Weber, Q. Lin, D. Gangloff, A. Bylinskii, B. Braverman, A. Kawasaki, C. Raab, W. Kaenders, and V. Vuletic, "Passive intrinsic-linewidth narrowing of ultraviolet extended-cavity diode laser by weak optical feedback," *Opt. Express* **22**, 11592–11599 (2014).
10. S. Mieda, N. Yokota, W. Kobayashi, and H. Yasaka, "Ultra-wide-bandwidth optically controlled DFB laser with external cavity," *IEEE J. Quantum Electron.* **52**, 1–7 (2016).
11. W. Lewoczko-Adamczyk, C. Pyrlík, J. Häger, S. Schwertfeger, A. Wicht, A. Peters, G. Rebert, and G. Tränkle, "Ultra-narrow linewidth DFB-laser with optical feedback from a monolithic confocal Fabry-Perot cavity," *Opt. Express* **23**, 9705–9709 (2015).
12. T. Hieta, M. Vainio, C. Moser, and E. Ikonen, "External-cavity lasers based on a volume holographic grating at normal incidence for spectroscopy in the visible range," *Opt. Commun.* **282**, 3119–3123 (2009).
13. Z. Feng, L. Bai, N. Wang, L. Gao, B. Gao, and X. Zhang, "Narrow-linewidth tunable semiconductor lasers based on dual-lens external-cavity structure," *J. Lumin.* **33**, 1138–1142 (2012).
14. R. Wyatt and W. J. Devlin, "10 kHz linewidth 1.5  $\mu\text{m}$  InGaAsP external cavity laser with 55 nm tuning range," *Electron. Lett.* **19**, 110–112 (1983).
15. A. Biebersdorf, C. Lingk, M. Giorgi, J. Feldmann, J. Sacher, M. Arzberger, C. Ulbrich, G. Böhm, M. Amann, and G. Abstreiter, "Tunable single and dual mode operation of an external cavity quantum-dot injection laser," *J. Phys. D* **36**, 1928–1930 (2003).
16. S. Saliba and E. Scholten, "Linewidths below 100 kHz with external cavity diode lasers," *Appl. Opt.* **48**, 6961–6966 (2009).
17. B. Li, A. Yu, S. Luo, D. Xiong, X. Wang, and D. Zuo, "500 mW tunable external cavity diode laser with narrow line-width emission in blue-violet region," *Opt. Laser Technol.* **96**, 176–179 (2017).
18. M. Chi, O. Jensen, and P. Petersen, "High-power dual-wavelength external-cavity diode laser based on tapered amplifier with tunable terahertz frequency difference," *Opt. Lett.* **36**, 2626–2628 (2011).
19. D. Ding, X. Lv, X. Chen, F. Wang, J. Zhang, and K. Che, "Tunable high-power blue external cavity semiconductor laser," *Opt. Laser Technol.* **94**, 1–5 (2017).
20. M. Chi, O. Jensen, and P. Petersen, "Green high-power tunable external-cavity GaN diode laser at 515 nm," *Opt. Lett.* **41**, 4154–4157 (2016).
21. L. Nilse, H. J. Davies, and C. S. Adams, "Synchronous tuning of extended cavity diode lasers: the case for an optimum pivot point," *Appl. Opt.* **38**, 548–553 (1999).
22. Thorlabs, "Ruled Diffraction Grating," 2019, [https://www.thorlabschina.cn/newgrouppage9.cfm?objectgroup\\_id=8627](https://www.thorlabschina.cn/newgrouppage9.cfm?objectgroup_id=8627).
23. N. Olsson and N. Dutta, "Effect of external optical feedback on the spectral properties of cleaved coupled-cavity semiconductor lasers," *Appl. Phys. Lett.* **44**, 840–842 (1984).